IOPscience iopscience.iop.org

Home Search Collections Journals About Contact us My IOPscience

Ultraviolet luminescence of $ScPO_4$, $AlPO_4$ and $GaPO_4$ crystals

This article has been downloaded from IOPscience. Please scroll down to see the full text article.

2013 J. Phys.: Condens. Matter 25 385502

(http://iopscience.iop.org/0953-8984/25/38/385502)

View the table of contents for this issue, or go to the journal homepage for more

Download details:
IP Address: 213.175.108.33
The article was downloaded on 02/09/2013 at 13:23

Please note that terms and conditions apply.

J. Phys.: Condens. Matter **25** (2013) 385502 (6pp) doi:10.1088/0953-8984/25/38/385502

Ultraviolet luminescence of $ScPO_4$, $AlPO_4$ and $GaPO_4$ crystals

Anatoly N Trukhin[1], Krishjanis Shmits[1], Janis L Jansons[1] and Lynn A Boatner[2]

[1] Solid State Physics Institute, University of Latvia, 8 Kengaraga Street, LV-1063, Riga, Latvia
[2] Materials Science and Technology Division, Oak Ridge National Laboratory, Oak Ridge, TN 37831-6044, USA

E-mail: truhins@cfi.lu.lv

Received 13 June 2013, in final form 18 July 2013
Published 29 August 2013
Online at stacks.iop.org/JPhysCM/25/385502

Abstract

The luminescence of self-trapped excitons (STEs) was previously observed and described for the case of tetragonal-symmetry $ScPO_4$ single crystals. The subject band in this material is situated in the UV spectral range of ~210 nm or ~5.8 eV. In the present work, we are both expanding this earlier luminescence study and seeking to identify similar luminescence phenomena in other orthophosphate crystals, i.e., $AlPO_4$ and $GaPO_4$. These efforts have proven to be successful—in spite of the structural differences between these materials and $ScPO_4$. Specifically we have found that for $AlPO_4$ and $GaPO_4$, in addition to an α-quartz-like STE, there is a UV luminescence band that is similar in position and decay properties to that of $ScPO_4$ crystals. Potentially this represents an STE in $AlPO_4$ and $GaPO_4$ crystals that is analogous to the STE of $ScPO_4$ and other orthophosphates. The decay kinetics of the UV luminescence of $ScPO_4$ was studied over a wide temperature range from 8 to 300 K, and they exhibited some unusual decay characteristics when subjected to pulses from an F_2 excimer laser (157 nm). These features could be ascribed to a triplet state of the STE that is split in a zero magnetic field. A fast decay of the STE was detected as well, and therefore, we conclude that, in addition to the slow luminescence corresponding to a transition from the triplet state, there are singlet–singlet transitions of the STE. Time-resolved spectra of the slow and fast decay exhibit a small shift (~0.15 eV) indicating that the singlet–triplet splitting is small and the corresponding wavefunction of the STE is widely distributed over the atoms of the $ScPO_4$ crystal where the STE is created.

(Some figures may appear in colour only in the online journal)

1. Introduction

$ScPO_4$ has a tetragonal zircon-type structure, and this material is frequently grouped together with the rare-earth orthophosphates (particularly those in the second half of the transition series) as well as tetragonal YPO_4. The orthophosphates in the first half of the rare-earth transition series have the monoclinic monazite structure and have been considered as a host ceramic material for radioactive waste storage [1]. The unit cell of the $ScPO_4$ zircon structure consists of four formula units, where each phosphorus atom is bonded to four nearby oxygen atoms, and each of the Sc atoms is surrounded by eight oxygen atoms [2]. The self-trapped exciton (STE) in $ScPO_4$ was initially described by Trukhin and Boatner [3, 4]. It exhibits a luminescence band in the UV range situated at ~210 nm (~5.6–5.9 eV). This band is broad even at liquid helium temperature with a FWHM of ~0.7 eV. This luminescence is excited above the intrinsic absorption threshold at 6.93 eV, belonging to the low energy side of the band at 8.8 eV. The threshold obeys the Urbach–Toyozawa rule [3, 4] witnessed on direct creation of STEs. The specific nature of the triplet–singlet transitions was found for the STE luminescence in $ScPO_4$ based on the discovery of an effect related to triplet splitting in zero magnetic

 © 2013 IOP Publishing Ltd Printed in the UK & the USA

fields [3, 4]—i.e. a strong increase in the luminescence duration that is observed without a corresponding change in intensity. This luminescence is thermally quenched above 400 K [3, 4]. For a triplet state that is split in zero magnetic fields, the observation of faster components in addition to slow components is a characteristic feature. Since a slow component was clearly observed for the $ScPO_4$ STE luminescence, the identification and explanation of shorter components of the decay at liquid helium temperature is warranted. Additionally, since the details of the nature of the STE in $ScPO_4$ are still not fully understood, we have undertaken a search for similar luminescence effects in other orthophosphates—but with a crystal structure that differs from that of $ScPO_4$.

The materials $AlPO_4$ and $GaPO_4$ are orthophosphates with the α-quartz structure. In comparison with silicon dioxide α-quartz, the structure is a repetition of Al(Ga) and P tetrahedrons. For both $AlPO_4$ and $GaPO_4$ crystals, a self-trapped exciton was discovered [5, 6] that is similar to that of the self-trapped exciton of silicon dioxide α-quartz. The luminescence band of the STE is situated in the visible spectral range. One distinguishing property of self-trapped excitons in crystals with the α-quartz structure is the existence of two types of STE—one that is approximately parallel to the *c*-axis and another that is approximately perpendicular to the *c*-axis of the crystal. This STE is related to Si(Al, Ga)–O bond rupture with creation of a bond between such non-bridging oxygen and a bonding oxygen on the opposite site of the channel, characteristic for α-quartz structure [5, 6]. For SiO_2, $AlPO_4$ and $GaPO_4$ crystals, the thermal quenching parameters, related to the oxygen–oxygen bond strength [5, 6], are different, and a two-step thermal dependence of the intensity of the STE luminescence was observed with a corresponding thermal dependence of the STE luminescence polarization [6]. The polarization of the luminescence is weak when both STEs are not quenched, and after one type is quenched, the remaining STE polarization is high (∼60%). In the case of GeO_2 crystals with the α-quartz structure, both STEs have an equal thermal quenching parameter, and as result, the polarization of the STE luminescence is weak. The STE luminescence in crystals with the α-quartz structure is attributed to singlet–singlet and triplet–singlet transitions. The latter is evident through the effect of zero field splitting of the triplet state that exhibits a slow decay (∼1 ms at 80 K) and a singlet–singlet transition evidenced by the detection of a very fast component of the STE luminescence (∼2–3 ns). The estimated value of the singlet–triplet splitting of the STE in crystals with the α-quartz structure is on the order of 0.2 eV—consistent with an STE wavefunction that is spread over many atoms and not simply localized. The energetic yield of the STE luminescence in crystals with the α-quartz structure is relatively high, and a level of 25–30% of the absorbed energy of the ionizing irradiation is emitted through STE luminescence.

In the present work, an extended study of the UV luminescence of $AlPO_4$ and $GaPO_4$ crystals is carried out with the goal of comparing the results for these materials to those obtained previously for $ScPO_4$. These new studies have led to the discovery of a UV band in both $AlPO_4$ and $GaPO_4$ crystals, and the decay of the band at 210 nm is similar to that found for $ScPO_4$. Thus, while these result suggest that the UV luminescent STE in the orthophosphates is related to complex phosphate–oxygen ions, we should note that for the $AlPO_4$ and $GaPO_4$ crystals, we were able to detect the 210 nm band only under electron beam excitation—while for $ScPO_4$ it was possible to detect this band for different excitations i.e., using a hydrogen discharge source with a vacuum monochromator, an excimer F_2 laser (157 nm) and certainly under cathodoexcitation. Additionally, we carried out new studies of the fast luminescence of the STE in $ScPO_4$ that we were not able to perform in previous investigations because of technical problems, and we had found such a fast luminescence practically coinciding with the slow STE luminescence. This is consistent with a small singlet–triplet splitting of the STE.

2. Experimental details

Single crystals of $SCPO_4$ were grown using a flux method [7] in tightly covered platinum crucibles containing lead pyrophosphate as the flux. After soaking for 16 h at 1360 °C, the crucibles were cooled at a rate of 1 °C h^{-1} to 900 °C and then cooled directly to room temperature. The $PB_2P_2O_7$ flux was then dissolved in boiling HNO_3. The $SCPO_4$ single crystals had different dimensions that did not exceed ∼80 mm^2. The other orthophosphate samples investigated were hydrothermally grown pure $GaPO_4$ and either pure or Sc/Ga-doped $AlPO_4$ single crystals.

The F_2 laser (model PSX-100, manufactured by Neweks, Estonia) used here had a pulse energy of about 0.5 mJ with a duration of 5 ns. The F_2 laser light was passed through a copper tube filled with flowing nitrogen. The excitation laser (2 × 2 mm^2 beam) was located 1 m from the sample. Crystalline silicon dioxide (α-quartz) with a low level of luminescence was used as a window to pass the excitation laser light, and the measurements were carried out with the use of a helium refrigerator. The temperature range in this case was 8–300 K. Luminescence detection was performed using a grating monochromator with a photomultiplier tube (H6780-04) with a 50-Ω resistive load. Optical filters were employed for reducing the laser light for luminescence detection, and an oscilloscope (Textronic TDS 2022B) was utilized for obtaining the decay curves. Each curve was averaged over 128 pulses. The time-resolved spectra were measured by recording the decay curve for each point of the PL spectrum over two time ranges—one in the ns range and the other in the μs range. The measured curves are shown in the figures 'as recorded'—therefore, they directly reflect the error level. The discharge of the excimer laser produces a strong stray current in the measurement circuit, that distorts the signal for a short time duration. A pulsed beam of 6 kV electrons was used for the CL and time-resolved experiments, and the frequency of the 0.1 μs pulses was controlled in the 50 Hz–20 kHz range. A double-grating monochromator was used to analyze the cathode luminescence spectrum, and the luminescence-kinetics curves were collected during

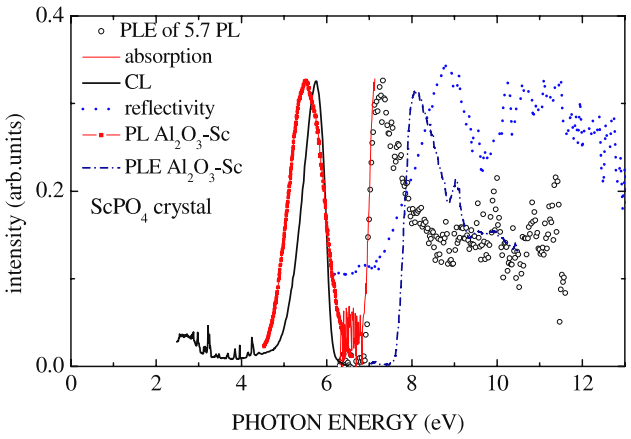

Figure 1. Optical spectra of $ScPO_4$ crystals in the intrinsic absorption range. PLE—photoluminescence excitation spectra, PL—photoluminescence spectra. CL—cathodoluminescence spectra. The spectra of Al_2O_3–Sc are reproduced from [8] for comparison.

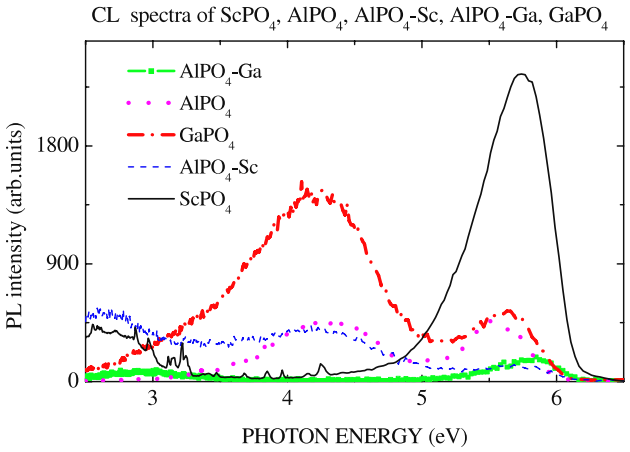

Figure 2. Comparison of cathodoluminescence spectra in different orthophosphates at 293 K. It is seen that the UV band is present in all of the measured orthophosphates.

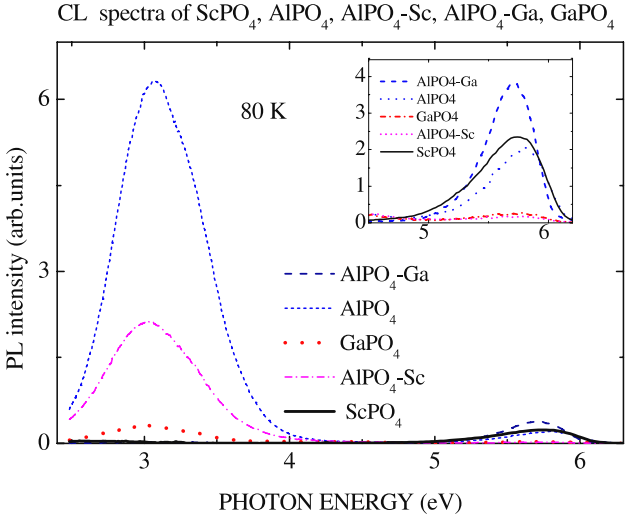

Figure 3. Comparison of cathodoluminescence spectra in different orthophosphates at 80 K. The visible luminescence of $AlPO_4$ and $GaPO_4$ crystals is similar to that of a silicon dioxide α-quartz crystal.

20 min of irradiation with a multichannel analyzer. A photomultiplier tube with an S20 photocathode was used. A tungsten x-ray tube (10 mA, 40 kV) was utilized to excite the photoluminescence spectra. Additionally, optical reflection spectra were measured using a vacuum monochromator and a windowless discharge from a hydrogen light source. The reflections were measured with respect to a gold mirror. For luminescence spectra measurements also a CCD with the Andor monochromator was used.

3. Results

The luminescence spectrum (cathodoluminescence), photoluminescence excitation (PLE) spectrum, absorption spectrum (in the range of the intrinsic threshold), and optical reflection spectra are presented in figure 1. It is shown that the PL at ~210 (~5.75 eV) is excited exactly in the range of intrinsic absorption of $ScPO_4$ at 6.93 eV [3, 4]. The decrease in the PLE above 7.5 eV can be related to a decrease in the penetrations depth, and it coincides with the position of the intrinsic absorption band at 8.8 eV (as estimated using the reflection spectrum). This intrinsic band apparently belongs to an exciton because of the low electric photoconductivity with respect to higher energy [3]. For comparison, we have also presented the PL and PLE of Al_2O_3 doped with scandium [8]. There is a PL band at 5.5 eV that starts just below the intrinsic absorption threshold of sapphire (~9 eV [8]).

Believing initially that, in fact, the UV band is associated with scandium, we decided to measure the luminescence of another orthophosphate material—i.e., berlinite ($AlPO_4$) doped with scandium. We found UV luminescence, however, not only in $AlPO_4$ doped with scandium but observed an even more intense UV band in pure $AlPO_4$. Accordingly, any correlation with the presence of Sc in alumina is apparently coincidental. We found a UV band both under F_2 laser and cathodoexcitation; however, since the intensity of the luminescence was quite small under F_2 laser excitation, we subsequently performed a series of cathodoluminescence measurements using other orthophosphates and compared the results to the UV luminescence observed for $ScPO_4$ (see figure 2). The data presented in figure 2 show that all of the studied orthophosphates exhibit a UV band in cathodoluminescence. The spectra measured at 80 K are presented in figure 3. In the samples of $AlPO_4$ and $GaPO_4$, there is an increased intensity of the 'normal' STE in the visible range, and the UV luminescence persists in all of the samples. It is known that the decay of the UV luminescence of $ScPO_4$ changes on cooling from a time constant of about 0.1 μs at 290 K to 3–4 μs at 80–65 K [3, 4], and the decay kinetics curves obtained at low temperature are presented in figure 4.

In all of the measured orthophosphates, the UV band kinetics changed in a similar way as a function of the temperature. By carrying out a check of the

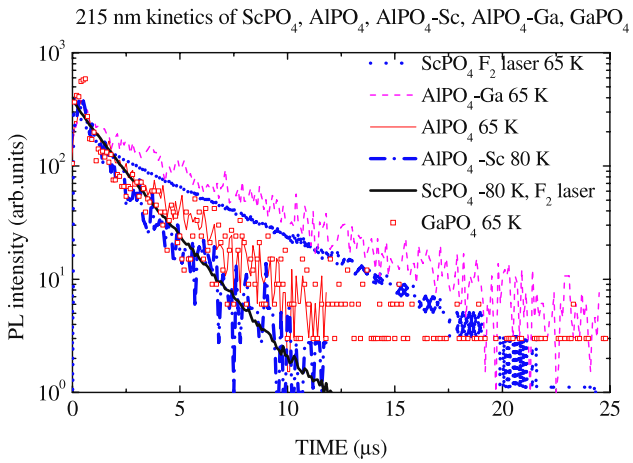

Figure 4. Comparison of cathodoluminescence decay kinetics of the UV band in different orthophosphates. For $ScPO_4$ the decay kinetics for excitation with an F_2 laser are presented at $T = 65$ K. It is seen that the decay kinetics are similar at corresponding temperatures for the measured samples.

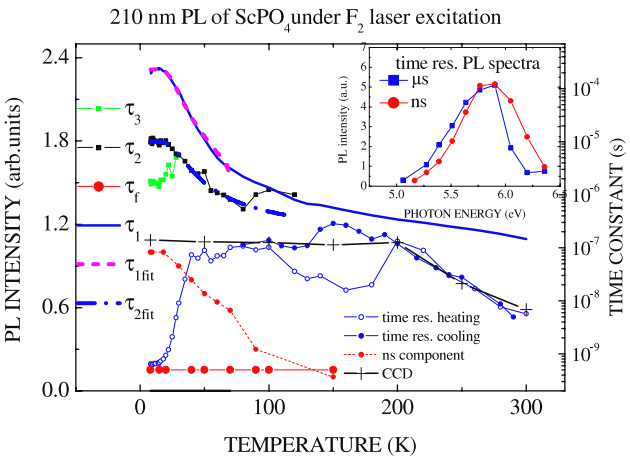

Figure 5. Temperature dependences of the decay time constant (τ) and intensity of the UV luminescence of $ScPO_4$ excited with pulses from an F_2 excimer laser (157 nm). The inset shows time-resolved spectra for the ns and μs ranges at 80 K. $\tau_{1fit} = \tau_{SLOW}$ and $\tau_{2fit} = \tau_{FAST}$—temperature dependences of the decay time constant are calculated with expressions (3) and (4).

cathodoluminescence signal using a plate of indium covered with orthophosphate acid, we found that even an indium surface covered with orthophosphate acid (like that used for soldering) provides a cathodoluminescence band at 210 nm with a materials decay kinetics similar to those noted previously—indicating that the UV band at 210 nm is characteristic of the presence of an orthophosphate.

We have performed a study of the decay kinetics of the $ScPO_4$ UV luminescence over a wide range of temperature under the excitation of an F_2 excimer laser at 157 nm (see figure 5). Besides the previously noted slow component of decay (∼0.2–0.3 ms), we have now obtained three additional decay components. It should be noted that using another detection system—i.e., photon counting instead of a direct measurement of the current of the PM using an oscilloscope, we observe a slow component on the order of 10 ms. This current regime does not permit the detection of such a long component distributed over time, and it is difficult to distinguish the signal from a zero level when using a relatively weak F_2 laser. Owing to this time-resolved intensity dependence on temperature, we observe a decrease in the signal below 40 K (see figure 5). This decrease is artificial because we were not able to record over the entire time range. The actual PL intensity dependence on temperature corresponds to signals obtained with a CCD and the Andor monochromator. There are no real changes in intensity below 40 K figure 5, and a flat line is observed.

An estimate of the fast component response, based on the level of the detection limit, is 0.5 ns, and this component decay is independent of temperature. Two other decay components are in the μs time range. At 8 K, the corresponding time constants are 1.5 and 10 μs. The latter decreases on heating while the other component increases on heating, probably due to the disappearance of corresponding transitions. Both components merge at 25 K. These three decay components are assigned to a triplet state splitting in zero magnetic fields, as noted previously [3]. In the inset of figure 5, the time-resolved spectra are shown for both the slow μs component and the fast ns component. Both components produced practically coinciding spectra. The spectrum for the ns component is shifted (see the figure 5 inset) to higher energy—about 0.1–0.2 eV. This shift potentially corresponds to the singlet–triplet splitting of the STE in $ScPO_4$.

4. Discussion

We have obtained new data on the spectral–kinetic properties of the STE UV luminescence in $ScPO_4$. We have identified similar UV luminescence in other orthophosphate crystals i.e., $AlPO_4$ and $GaPO_4$ in spite of the structural differences between these materials and $ScPO_4$. This represents an additional STE in $AlPO_4$ and $GaPO_4$ crystals which is analogous to the STE of $ScPO_4$. It exists beside previously studied STE in $AlPO_4$ and $GaPO_4$ crystals analogous to that of SiO_2 α-quartz [5, 6], possessing a luminescence band in the visible range of the spectra. The STE of α-quartz structured crystals is related to oxygen–oxygen bond creation, when the exciton is self-trapped. Such an exciton was not found in the structure of $ScPO_4$. The STE in $ScPO_4$ is related to the PO_4 molecular ion and therefore the second STE in $AlPO_4$ and $GaPO_4$ crystals is related to the PO_4 molecular ion as well. Possibly, such UV luminescence is a property of orthophosphates. Observation of the band at 210 nm after soldering, with use of orthophosphate acid, is an argument for that. However, the probability of such STE existence in $AlPO_4$ and $GaPO_4$ crystals is small, perhaps because of the high efficiency of exciton self-trapping in the style of α-quartz. Therefore, this $ScPO_4$-like STE we observe only in specific excitation with an electron beam, figure 2.

We have obtained new data on STE in $ScPO_4$ crystals. Specifically, in addition to the known [3] slow component of decay, we have obtained results for a fast (ns) component and two slower components (1.5 and 10 μs). The slow component

decay is somewhat faster than the value obtained previously (10 ms)—presumably related to technical factors as noted in section 3. The fast (ns) component of the decay is ascribed to singlet–singlet transitions and the slow components to triplet–singlet transitions of the STE. It is difficult to determine exactly a value of the decay that is not affected by temperature, since in the range of temperatures below 200 K (where the intensity is practically unchanged), the decay time constant is monotonically increasing on cooling. Therefore, we can assume that at 150 K there is no additional component of decay with the exception of the fast component, and we can estimate the decay time constant at 100 K (1.5 μs) where the occupation of the triplet state sublevels occurs uniformly with temperature. The value of 1.5 μs exactly coincides with one of the decay components at 8 K. This last component of the decay exhibits an unusual temperature dependence on heating. It becomes slower on heating and then merges with a 10 μs component. The second component exhibits a usual thermal dependence—accelerating on heating and disappearing at 100 K. Accordingly, the behavior of the triplet state STE splitting is normal for the case of splitting in zero field [9, 10], where in addition to the slow component (due to long a long residence on $M = |0\rangle$), both of the sublevels $M = |-1\rangle M = |1\rangle$ are radiative and decay at 8 K. (They possess two components in the μs range where the sublevel is uniformly occupied.) Effects of the 1.5 μs component slowing on heating may be due to occupation from corresponding sublevels merging with another triplet sublevel that is responsible for the 10 μs component.

The shift between the time-resolved bands corresponding to the fast and slow components evidently corresponds to a singlet–triplet splitting of the STE in $ScPO_4$. This shift is small (0.1–0.2 eV) and would, therefore, correspond to large spatial dimensions of the wavefunction of the STE.

An analytical model describing the peculiarities of the luminescence decay kinetics was developed in [9] for the case of quartz and GeO_2 cathodoexcitation. This model is based on previous investigations of the STE in alkali halides (see references in [9]). At low temperatures, when the spin–lattice relaxation is frozen, the exchange between the ZFS sublevel of the triplet state is 'frozen'. Both values of the zero field splitting D and E [9] could be real for the UV luminescence of $ScPO_4$, and the observation of two components in the μs range of time may show the existence of zero field splitting with two radiative sublevels. Increasing the temperature merges both sublevels—evident in figure 5 as the merging of τ_2 and τ_3. The sublevels occupation could then be expressed using corresponding kinetic equations [9, 10], written for the general case:

$$\frac{dn_a}{dt} = -\left(\frac{1}{\tau_a} + \omega_a\right) n_a + \omega_b n_b; \quad (1)$$

$$\frac{dn_b}{dt} = -\left(\frac{1}{\tau_b} + \omega_b\right) n_b + \omega_a n_a \quad (2)$$

where n_i $(i = a, b)$ and τ_i correspond to the population and the radiative time constants of each sublevel, and ω_i is the non-radiative transition rates from level i to the other level. From these kinetic equations, two exponential components can be obtained with two decay time constants τ_S and τ_F, where the temperature dependence is given by the following expressions, [9, 10]:

$$\frac{1}{\tau_S} = \frac{1}{2}\left\{\left(\frac{1}{\tau_a} + \frac{1}{\tau_b} + \omega_a + \omega_b\right) - \left[\left(\frac{1}{\tau_a} - \frac{1}{\tau_b} + \omega_a - \omega_b\right)^2 + 4\omega_a\omega_b\right]^{1/2}\right\}; \quad (3)$$

$$\frac{1}{\tau_F} = \frac{1}{2}\left\{\left(\frac{1}{\tau_a} + \frac{1}{\tau_b} + \omega_a + \omega_b\right) + \left[\left(\frac{1}{\tau_a} - \frac{1}{\tau_b} + \omega_a - \omega_b\right)^2 + 4\omega_a\omega_b\right]^{1/2}\right\}. \quad (4)$$

As in previous cases [9, 10], the best fitting procedure was obtained by introducing the Orbach process. If a low-lying excited spin manifold exists near the ground-state manifold, the Orbach process dominates the relaxation pathway. Given an excited spin manifold at an energy E_a above the ground-state manifold, the spin system is promoted into the excited spin manifold by the absorption of a phonon and returns to another spin state of the ground-state manifold as another phonon E_b of slightly different energy is emitted. For low temperatures, the Orbach process relaxation rate varies exponentially with inverse temperature: $\nu_i \exp(-E_i/(k_B)T)$, where k_B is the Boltzmann constant, ν_i are the temperature independent rates of non-radiative transitions, and E_i is the energy separation between each sublevel and the additional state. If the two sublevels are degenerate, then $\nu_b/\nu_a = 2$, [9]. From a fitting of the experimentally determined data, the resulting dependences $\tau_S = \tau_1$ and $\tau_F = \tau_2$ are obtained and presented in figure 5 with the appropriate parameters given in the caption. A fitting for τ_3 was not performed. We should emphasize that the fitting procedure is good over a wide range of ν_i and E_i. (The larger the value of E_i, the smaller the value of ν_i. Thus, some independent source of the values of those parameters is required.) The nature of the ZFS is determined by the crystal-field, spin–orbit interaction, and spin–spin interactions. The parameters obtained for the UV luminescence of $ScPO_4$ are: $\tau_a = \tau_1 = 2 \times 10^{-4}$ s; $\tau_b = \tau_2 = 10^{-5}$ s; $\nu_a = 10^7$ s^{-1}; $\nu_b = 6 \times 10^7$ s^{-1} being close to the relation $\nu_b/\nu_a = 2$; $E_a = 0.013$ eV; $E_b = 0.011$ eV. τ_3 was not used for the simulation because it merges together with τ_2. The E_i values are high, but are in agreement with those known from the literature (see e.g. [9, 10]). The difference is too big for estimation of zero field splitting parameters of triplet state D and E. For that, ODMR studies of STE in $ScPO_4$ are needed.

5. Conclusions

A UV band at 210 nm was observed in several orthophosphate crystals that is ascribed to the PO_4 complex. The STE in $ScPO_4$ exhibits singlet–singlet and triplet–singlet transitions.

The triplet state of the STE is split in zero magnetic fields producing two radiative sublevels and one metastable sublevel. The singlet–triplet splitting of the STE is about 0.15 eV, indicating that the corresponding wavefunction is spatially distributed with an electron component on the Sc ions and a hole component on the PO_4 complex. Observations of the UV band in other orthophosphates similar to the case of $ScPO_4$ lead us to assume that the PO_4 complex ion is responsible for the STE. The large spatial dimensions of the wavefunction lead to the hypothesis that the PO_4 complex is responsible for the hole component of the STE and the electron component is distributed in space. In $AlPO_4$ and $GaPO_4$ crystals, the center responsible for UV luminescence is apparently similar to the case of the STE in $ScPO_4$.

Acknowledgments

This work is supported by the Latvian Council grant 2013.10-5/014 as well as Latvian National program 'IMIS'. Research at the Oak Ridge National Laboratory (LAB) was supported by the US Department of Energy, Basic Energy Sciences, Materials Sciences and Engineering Division. The samples of $AlPO_4$ and $GaPO_4$ were presented by Professor J Valbis.

References

[1] Boatner L A, Beall G W, Abraham M M, Finch C B, Huray P G and Rappaz M 1980 *Scientific Basis for Nuclear Waste Management* ed C J Northrup (New York: Plenum) p 289

[2] Milligan W O, Mullica D F and Boatner L A 1982 *Inorg. Chim. Acta* **60** 39

[3] Trukhin A N and Boatner L A 1996 *Mater. Sci. Forum* **239–241** 573

[4] Trukhin A N and Boatner L A 2000 *Proc. 5th Int. Conf. on Inorganic Scintillators and their Applications* ed V Michailin (Moscow: University of Moscow) p 697

[5] Trukhin A N 1994 *Solid State Commun.* **90** 761

[6] Trukhin A N 1996 *Mater. Sci. Forum* **239–241** 531

[7] Boatner L A 2002 Structure and properties of monazite, pretulite, and xenotime *Phosphates: Geochemical, Geobiological, and Materials Importance* (*Reviews in Mineralogy and Geochemistry* vol 48) ed J M Hughes, M Kohn and J Rakovan (Chantilly, VA: Mineralogical Society of America & the Geochemical Society)

[8] Kirm M and Zimmerer G 1999 *Phys. Rev.* B **60** 502

[9] Itoh C, Tanimura K and Trukhin A N 1996 *Nucl. Instrum. Methods Phys. Res.* B **116** 72

[10] Trukhin A N, Kink M, Maksimov J and Kink R 2003 *Solid State Commun.* **127** 655